XMM-Newton CCF Release Note

XMM-SOC-CAL-SRN-0299

Coefficients of the Rate-Dependent PHA (RDPHA) correction based on the derivative spectra

M. Guainazzi

7 February 2013

1 CCF components

Name of CCF	VALDATE	EVALDATE	Blocks changed	XSCS flag
EPN_CTI_0027.CCF	2001-01-01	2020-01-01	RDPHA_DERIV	NO

The overall re-calibration of the energy scale in EPIC-pn Fast Modes requires the simultaneous correction of two effects: a) X-ray Loading (XRL; Smith 2004); b) and a residual positive correlation between the energy scale and the source count rate.

Currently, the latter effect is modelled through the so-called "Rate-Dependent CTI" (RD-CTI; Guainazzi et al. 2008). This correction is applied to the PI column of the calibrated event list as a gain factor, G ($G \equiv E_{original}/E_{corrected}$). The dependence of G on the total count rate is calculated by applying a XSPEC `gain fit` to the 1.5–3 keV spectra of a wide sample of different continuum-dominated sources. The `gain fit` calculates the linear term of the gain (assuming a constant 0 offset) required to minimise the residuals in this energy band. This factor is applied in the SAS by the task `epfast`, which calculates G corresponding to each of the `RAWX` column in intervals of `timebinsize` seconds.

There are several potential issues with this approach. The results of this technique are in principle dependent on the astrophysical nature of the calibration sources, and on the astrophysical model employed to fit their spectra in PI space. Moreover, `gain fit` applies an energy shift to the instrument response rather than to the data. It therefore performs a different function to what is required to calibrate the rate-dependence of the energy scale. Finally, a proper energy scale correction should be calibrated in PHA space, before the gain is applied.

In this Release Note, we describe an alternative approach, based on fitting the peaks of the spectral *derivative in PHA space*. A preliminary calibration embedded in the parameters of `EPN_CTI_0027.CCF` is also presented here. A refinement of this calibration is likely once this algorithm is implemented in the SAS.

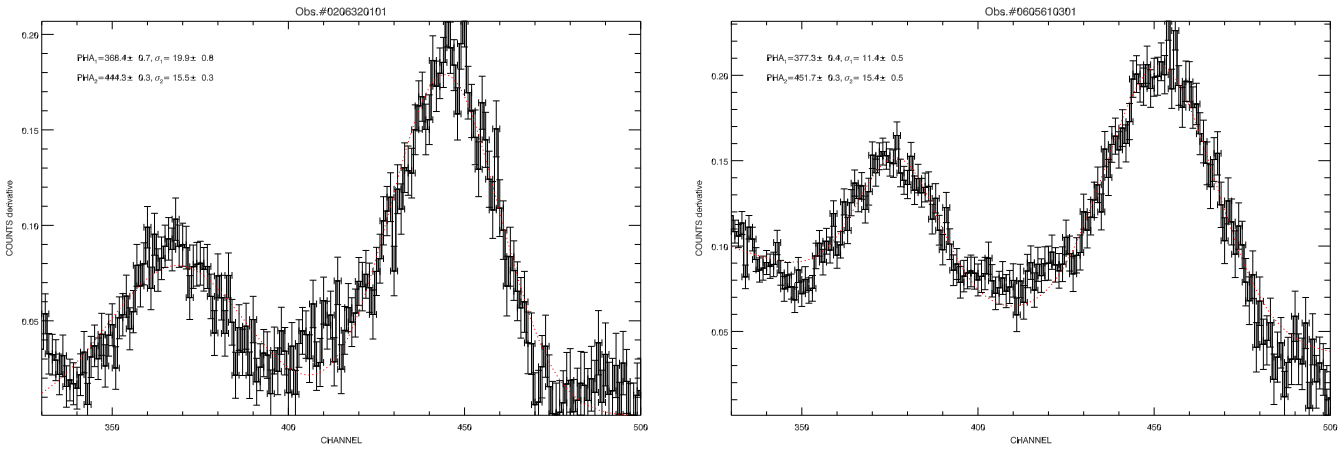

Figure 1: Examples of derivative PHA spectra. The *red dashed* line indicates the best-fit.

2 Changes

The rationale of the proposed method relies on the fact that the strongest gradients in an EPIC-pn effective area occur at the location of the Si (≃1.8 keV) and Au (≃2.2 keV) edges. The exact position of these edges is a sensitive measurement of the energy scale. However, a direct fit of the edges in the PHA spectra is uncertain, and leads to inaccurate measurements due to the resolution of the EPIC-pn cameras. The situation changes radically if one works on the derivative of the spectrum in PHA space, δ, defined as:

$$\delta(PHA, \Delta PHA) \equiv \frac{|C_i(PHA) - C_i(PHA + \Delta PHA)|}{C_i(PHA) + C_i(PHA + \Delta PHA)}$$

Two examples of PHA spectral derivative around the instrumental edges are shown in Fig. 1. The two peaks can be robustly fit with a simple phenomenological model constituted by a power-law and two Gaussian profiles. The peak of the Gaussian functions as a function of the number of shifted electrons, N_e, is shown in Fig. 2. N_e is defined as:

$$N_e = \frac{\Sigma_{i=1}^{N_p} E_i}{N_{pixels} \times T_{exp} \times 3.6}$$

where E_i is the *PHA* value of the i-th photon, N_{pixels} is the number of pixels of the column whence each spectrum was extracted, N_p is the number of detected photons, T_{exp} is the exposure time and the factor 3.6 (in eV) represents the energy required to produce an electron-hole pair. In Fig. 2 the best-fit parameters and functions are shown, when the data are fit with a linear function of the logarithmic abscissa: PHA=c+$d \times \log(N_e)$. For the Silicon (Gold) edge: c=351 ± 2 (420.5 ± 1.6), d=7.5 ± 1.0 (10.0 ± 0.6). These values of d (together with their 1-σ uncertainty) are included in `EPN_CTI_0027.CCF`.

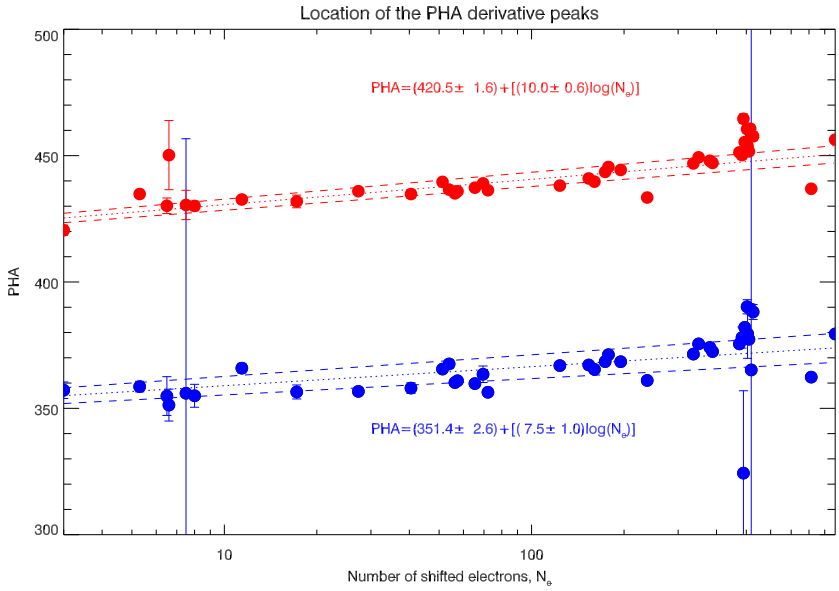

Figure 2: Si- and Au-peaks in the PHA derivative spectra as a function of N_e. Errors are at the 1σ level. The *dotted lines* represent the best-fit function as specified in the *inset labels*. The *dashed lines* represent the envelope corresponding to the 1σ confidence level on the best-fit parameters.

3 Scientific Impact of this Update

There is no impact for SAS users running the SAS with default parameters. The new extension is not accessed by the SAS, unless a specific parameter in `epevents` in used: `withrdcti=Y`. We have tested the backward-compatibility of the CCF, by running `epproc` twice on the ODF of the EPIC-pn Timing observation of RSOph (Obs.#0410180101; see Sect. 4.1): a first time with the public CCF suite available at the time this Release Note was written; a second time with the same suite augmented by `EPN_CTI_0027.CCF`. Any randomisation was switched off by setting: `randomizeposition=no`, and `randomizeenergy=no` as inputs of `epproc`. The `PHA` columns in the resulting event lists are identical.

This method is intended to ultimately supersede the RDCTI currently implemented in the SAS through `epfast` and the `RATE_DEPENDENT_CTI` extension of the `EPN_CTI` CCF. The RDPHA *requires* the XRL correction to be also properly calibrated. This correction is already supported by the SAS as of its version #12, although it is currently inactive because the parameters of the associated CCF (`EPN_REJECT_0006.CCF`) are dummy. A Release Note discussing the calibration of this effect is in preparation: (Guainazzi & Smith, "Calibration of the spectral impact of X-ray Loading in EPIC-pn Timing Mode", XMM-CCF-REL-0296).

4 Estimated Scientific Quality

With the PHA derivative algorithm, only differences in PHA space can be measured. In the following, we will assume that the data points with the lowest N_e are not affected by any RDCTI, and use a weighted average of the slopes obtained for the two instrument edges: d_{RDCTI} =9.3. The calibration of the RDPHA has been scientifically validated using two metrics:

- comparing the centroid energy of more than 10 emission lines measured in the spectrum of the recurrent symbiotic Nova RSOph during its most recent outburst (February 2006; Nelson et al. 2008, Ness et al. 2009) with the expected laboratory energy
- evaluating the residuals around the Si and Au instrumental edges against a physically motivated continuum model in a sample of obscured X-ray Binaries (XRBs)

Data were reduced with a in-house version of `epchain` having the XRL correction activated. Prior to running `epevents`, the `PHA` column in the event list generated by `epframes` was modified through an IDL script implementing the new RDCTI calibration. In Sect. 4.1 we will show the effect of randomising of the `PHA` column after the application of the RDCTI. Spectra were extracted from a 19 pixel box in `RAWX` coordinates around the boresight column (determined independently for each observation). Background subtraction was applied, using spectra extracted from a 4 pixel wide box in `RAWX` coordinates around `RAWX`=4. Instrument responses were generated for each observation through `rmfgen` and `arfgen` using the public version of SASv12.

4.1 RS Oph

We employed a phenomenological spectral model composed by two bremsstrahlung component and as many Gaussian profiles (16) as required by the condition that the addition of a further emission line does not improve the fit at a confidence level $\geq$90%. The best-fit centroid energies were compared to the wavelength of the closest transition (according to the ATOMDB database; Foster et al. 2012) in a list including the following ones: NVII-Lyα, OVII-Hα(r), OVIII-Lyα NeIX-Hα(r), NeX-Lyα, MgXI-Hα(r), FeXXIV-Lyα, MgXII-Lyα, SiXIII-Hα(r), SiXIV-Lyα, SXV-Hα(r), SXVI-Lyα, ArXVII-Hα(r), ArXVIII-Lyα, CaXIX-Hα(r), CaXX-Lyα, FeI-Kα, FeXXV-Hα(r), FeXXV-Hα(i), FeXXV-Hα(f), FeXXVI-Lyα, FeXXVI-Lyβ (not all of them are detected in RSOph). We apply to the line energy the velocity shifts as measured in high-resolution spectra (cf. Tab. 2 in Ness at al. 2009), although they make a negligible difference to the results presented hereafter.

Fig. 3 summarises the results of this comparison. Using the current best-calibration of the XRL (data points labelled "offset" in Fig. 3; Guainazzi et al., in preparation) yields a significant improvement in the accuracy of the energy reconstruction, most notable below $\simeq$2 keV. The measured energy accuracy is within 10/25/20 eV for E$\leq$2 keV, 2 keV<E$\leq$ 4 keV and E>4 keV, respectively.

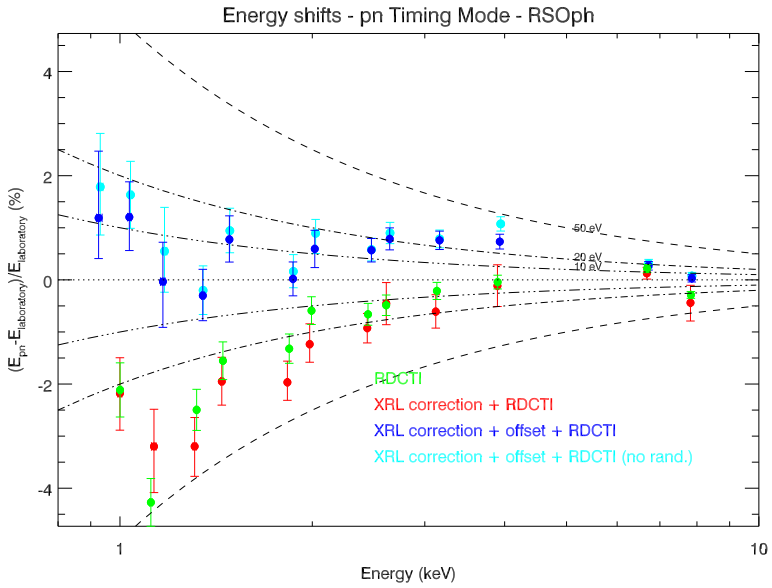

Figure 3: Percent difference between the line energy measured in the EPIC-pn Timing Mode spectrum of RS Oph (Obs.#0410180101) and the laboratory energy of the closest transition as a function of the latter. The *colours* indicate different calibration processes: *green*: RDCTI only; *red*: XRL($a = 0$) and RDCTI; *cyan*: XRL($a = -6.9$ ADU), and RDCTI without `PHA` randomisation; *blue*: the same as *cyan* with randomisation. The a parameter is the linear offset in the XRL versus PHA shift relation. This parameter in included in `EPN_REJECT_0007.CCF`. A Release Note discussing its calibration is in preparation: Guainazzi & Smith, "Calibration of the spectral impact of X-ray Loading in EPIC-pn Timing Mode", XMM-CCF-REL-0296. The *dotted*, *dashed-dotted*, and *dashed lines* represent the 10, 20, and 50 eV difference locii, respectively.

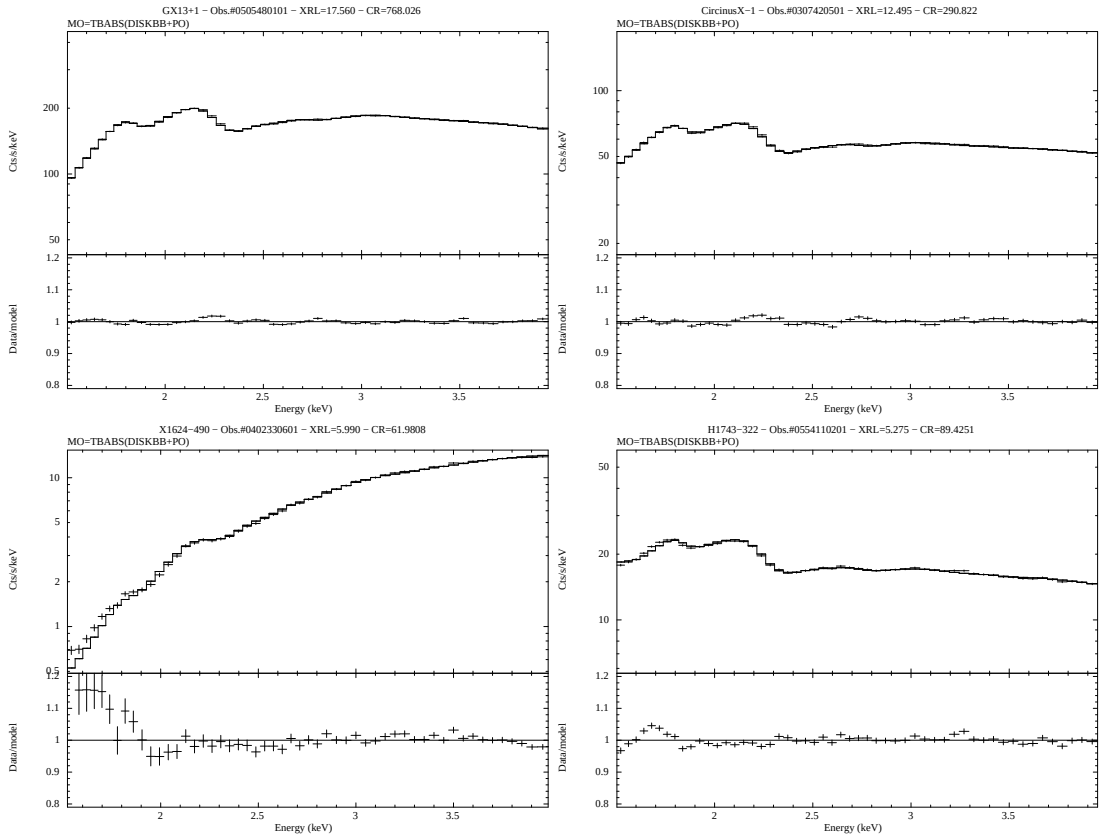

Figure 4: Spectra (*upper panels*) and residuals in data/model ratio (*lower panel*) on 4 objects extracted from the obscured X-ray binary sample.

4.2 Obscured X-ray binaries

In Fig. 4 we show the residuals against a standard accretion disk + corona fit on a representative sub-sample of 4 obscured X-ray binaries extracted from a larger sample of 18 observations (cf. Sect. 6 in Guainazzi et al. 2012) when the energy reconstruction method based on the RDPHA is applied. The residuals at the instrumental edges are within ±3%.

We stress that this result is *totally independent* of the RDCTI calibration algorithm. This is not the case with the current algorithm, which is based on finding the G-factor minimising the residuals exactly in the 1.5–3 keV energy band. Smooth residuals in this energy range are therefore automatically obtained. The new calibration works on the derivative spectra in PHA space. The smooth residuals obtained on the spectral fitting are therefore a *bona fide* independent test of the calibration quality.

5 Test procedures and results

This new CCF component is being tested together with `epevents` versions ≥6-45. The results of these tests will be published in the Science Validation Report of SASv13, as well as in an update version of Guainazzi et al. (2012).

6 References

Foster A., et al., 2012, ApJ, 756, 128
Guainazzi M., et al., 2008, XMM-CCF-REL-0248
(available at: `http://xmm2.esac.esa.int/docs/documents/CAL-SRN-0248-1-0.ps.gz`)
Guainazzi M., et al., 2012, XMM-SOC-CAL-TN-0083
(available at: `http://xmm2.esac.esa.int/docs/documents/CAL-TN-0083.pdf`)
Nelson et al., 2008, ApJ, 673, 1067
Ness J.-U., et al., 2009, AJ, 137, 3414
Smith M., 2004, XMM-SOC-CAL-TN-0050
(available at: `http://xmm2.esac.esa.int/docs/documents/CAL-TN-0050-1-0.ps.gz`)